4 Tropical Boundary Layers

The atmospheric boundary layer is the layer of air adjacent to the surface that is influenced by the surface on time scales of minutes to hours. It is usually dominated by turbulent transport, with the exception of calm nights over land in which the cooling from below and the absence of mean wind suppresses any turbulence. The turbulence may be generated by shear instabilities as air passes over rough surfaces, and/or by convection when there is a buoyancy source at the surface. Turbulent boundary layers often have well defined upper boundaries above which the turbulence ceases abruptly, and air from the overlying quiescent atmosphere is turbulently entrained into the boundary layer.

Boundary layer turbulence is the essential means by which the atmosphere and the underlying surface communicate, and the rates of transfer of heat, moisture, momentum, aerosols, and trace gases between the surface and the atmosphere are controlled by the turbulence. It is therefore essential to understand boundary layers for understanding virtually everything that happens in the tropical atmosphere. For example, when we come to discuss tropical cyclones we will see that their intensity and structure is mostly controlled by enthalpy and momentum fluxes between the atmosphere and ocean.

Over land, the character of the boundary layer is strongly influenced by the diurnal cycle of solar radiation, but even over the sea there are subtle diurnal variations owing to direct absorption of sunlight in the atmosphere and by clouds, and if there is little surface wind, by variations in the skin temperature of the ocean.

Water plays several important roles in boundary layer physics. Because its molecular weight is less than a suitably defined mean molecular weight of the other constituents of air, moist air is less dense than dry air at the same pressure and temperature. Thus water evaporating into the atmosphere from the surface is a source of buoyancy and can be the dominant source over warm oceans. Much of the boundary layer over tropical oceans contains cloud, and the phase changes of water – including condensation and evaporation of cloud droplets and the fall and evaporation of rain – can have important effects on the structure and turbulent properties of the boundary layer. Moreover, the radiative effects of clouds are substantial, particularly in the case of stratocumulus-topped boundary layers, whether the cloud cover can be close to 100%.

4.1 Some general principles

For the purposes of this book, we will consider only turbulent boundary layers and pass over the problem of laminar boundary layers, which can sometimes be found over land or cold water under very low wind conditions. We will consider all of the earth's surface to be thermodynamically and mechanically "rough", in the sense that fluxes to and from the surface are not rate-limited by molecular diffusivities. Thus none of the scaling laws we will review here depend on molecular diffusivities. This makes atmospheric boundary layers fundamentally different from other boundary layers found in literature on, e.g. Raleigh convection, pipe flow, aerodynamics, and other applications.

In the case of clear or stratocumulus-topped boundary layers, the whole layer may be considered to be filled with turbulence, but in trade cumulus boundary layers the turbulence is mostly confined to the cumulus clouds and the cloud-free air in between may be largely free of small scale turbulence. Even so, we will consider the cloud-bearing layer to be part of the overall boundary layer. In this case, the cumuli are important elements of the turbulent exchange between the surface and the atmosphere.

In regions experiencing deep convection, by the same reasoning, one might consider the whole troposphere to be a boundary layer, as convective turbulence is, as we have seen in previous chapters, and essential turbulent process in transferring energy, water, aerosols, and other trace constituents through the atmosphere. Nevertheless, by convention, we do not consider the whole layer containing deep convection to be a boundary layer.

It is important to be precise about the kinds of questions we ask about boundary layers. We might be interested in them for their own sake – for example, the nature of the turbulence itself, and its organization into geometric forms. On the other hand, our primary interest might be in how the boundary layer affects the free troposphere above it; for example, how it mediates the turbulent and radiative fluxes into the free troposphere from below. In the climate arena, most of the planet's albedo arises from clouds, and much of this is from boundary layer clouds, so here it is clearly essential to understand and be able to predict where and when cloud-topped boundary layers are present.

In thinking about the boundary layer as a system, it is important to be clear about which are the externally specifiable conditions and which are internally controlled conditions. For example, in the Prandtl convection problem explored in Chapter 2, section 2.3, the external conditions are the cooling rate applied to the fluid and the temperature and roughness of the surface; everything else, such as the turbulent velocities and time-mean vertical temperature profile, are internally determined. One can express the surface heat flux as the product of mean turbulent flow speed, the surface roughness, and the temperature gradient across some specified altitude range, and it becomes tempting to think that the surface flux is "caused" by the flow and the temperature gradient, but this would be misleading. As we shall see, surface fluxes in models are often parameterized as functions of a near-surface flow speed and gradients in quantities between the surface and some specified altitude. In reality, both the gradients and flow speeds are functions of more nearly external conditions such as internal cooling rates and surface roughness. Calculations of surface fluxes using parameterizations that involve gradients and flow speeds may have to be iterative, as both are functions of externally specifiable conditions.

In what follows we treat boundary layers of increasing complexity, aiming for simplicity and conceptual clarity.

4.2 Semi-infinite thermal and mechanical turbulent layers

Although clearly unrealistic, semi-infinite Boussinesq fluids in a constant gravitational field and bounded below by a rough, rigid surface are useful idealizations because they are controlled by a very limited number of parameters.

We have already derived, on dimensional grounds, velocity and buoyancy scales for a convective boundary layer driven by internal cooling and with no mechanical forcing (see Chapter 2). Here we follow the same strategy in deriving scales for a boundary layer driven entirely by mechanical forcing, with no thermal forcing; here all the turbulence is driven by shearing instabilities arising from flow deceleration near the mechanically rough lower boundary.

In the Prandtl convective system we specified a finite vertically integrated cooling rate that, in equilibrium, must also equal the total heat flux through the lower boundary. Here we do the mechanical equivalent by specifying a vertically integrated momentum flux per unit mass, M, that has dimensions L^2t^{-2} and can be thought of it as supplied by a vertically uniform, infinitesimal horizontal pressure gradient. In statistical equilibrium, the vertically integrated momentum sink must be balanced by a momentum flux through the surface, or equivalently, a surface stress. By convention, this surface stress per unit mass is denoted as u_*^2, where u_* is known as the *friction velocity.*

To avoid singularities, we introduce a mechanical roughness length z_0 below which molecular diffusion of momentum becomes important. Once again, the size of the turbulent eddies must scale with altitude, z. The velocity of the eddies scales as u_*, and the ensemble average wind shear must scale as $u_* z^{-1}$:

$$\frac{d\bar{U}}{dz} = \frac{1}{k} u_* z^{-1}, \tag{4.1}$$

where the constant factor k is called the von Kármán constant. Integrating (4.1) with altitude and taking $\bar{U} = 0$ at $z = z_0$ gives

$$\bar{U} = \frac{1}{k} u_* \ln\left(\frac{z}{z_0}\right). \tag{4.2}$$

The logarithmic increase of mean winds with attitude in mechanically forced boundary layers has been experimentally verified in a large number of settings. The von Kármán constant is based on fits of observed wind profiles to (4.2) and is a number close to 0.4.

What happens when there is both mechanical and thermodynamic forcing? We can begin by looking at the ratio of convective to mechanical turbulent velocity scales:

$$R = \frac{\left(zF_B\right)^{1/3}}{u_*}. \tag{4.3}$$

This ratio increases with height, so we might expect that at low levels shear driven turbulence dominates while at high levels the turbulence is driven mostly by convection. From (4.3) the altitude L at which the two velocity scales are roughly equal is given by

$$L = \frac{u_*^3}{kF_B}. \tag{4.4}$$

This length scale is known as the Obukhov length[1] after the Russian scientist who helped develop the theory of mechanically forced boundary layers that also have buoyancy effects. The von Kármán constant is included by convention. For our purposes, L can be regarded as the altitude above which convective turbulence dominates. In boundary layers that are both mechanically and convectively forced, we expect turbulence quantities to also scale with the nondimensional altitude z/L. Typical values of L range from 1 to 50 m, which is usually a reasonably small fraction of the total boundary layer depth in the tropics. Over tropical oceans, the top of the boundary layer is typically a few hundred meters, so it is usually the case that the bulk of the boundary layer is convectively driven.

The presence of both mechanical and convective forcing effective introduce a non-dimensional parameter into the problem; namely, the ratio of the altitude to the Obukhov length L. This requires us to modify (4.1) for the strictly mechanical boundary layer to

$$\frac{d\overline{U}}{dz} = \frac{1}{k} u_* z^{-1} \Psi_M \left(\frac{z}{L} \right), \tag{4.5}$$

where Ψ_M is some universal function, and likewise requires us to modify the strictly thermally forced boundary layer profile given by (2.54) to

$$g\beta \frac{d\overline{T}}{dz} = -c_1 F_B^{2/3} z^{-4/3} \Psi_T \left(\frac{z}{L} \right), \tag{4.6}$$

where Ψ_T is another universal function. These relations are the cornerstone of turbulent boundary layer theory, known as Monin-Obukhov similarity theory (Monin and Obukhov, 1954). The functions Ψ_M and Ψ_T must be determined empirically, through field measurements, but to reduce appropriately to the purely mechanical and purely thermal limits, they must obey $\Psi_M \left(L \to \infty \right) = 1$ and $\Psi_T \left(L \to 0 \right) = 1$. Moreover, we expect that near the thermal limit, momentum may behave more like a passive tracer while near the mechanical limit, temperature may act like a passive tracer; this hypothesis places more limits on the functional forms. Candidate functions derived from field experimental data (e.g. Businger and J. C. Wyngaard, 1971; Dyer, 1974) that meet these limits are

$$\Psi_M = \left(1 + 11 \left(\frac{z}{L} \right) \right)^{-1/3} \tag{4.7}$$

and

---

[1] Note that when boundary layers are thermally stable, F_B is negative. But by convention, the Monin-Obukov length is defined to be negative when F_B is positive. Since we will not be dealing with stable boundary layers here, we buck that convection and define L to be positive for convecting boundary layers.

$$\Psi_T = \left(1 + \frac{1}{13}\left(\frac{L}{z}\right)\right)^{-1/3}. \tag{4.8}$$

These relations are only valid for unstable boundary layers for which L (as we have defined it here) is positive.

We have thus far treated the atmosphere as a homogeneous gas. But particularly in the lower tropical atmosphere, water vapor variability makes an important contribution to the variability of specific volume. This can be seen in the definition of the virtual temperature given by (3.10) and repeated here:

$$T_v \equiv T\left(\frac{1 + r/\varepsilon}{1 + r}\right), \tag{4.9}$$

where r is the mass concentration of water vapor (mass of water per unit mass of dry air) often referred to simply as the *mixing ratio*, and $\varepsilon \equiv R_d / R_v \cong 0.622$ is the ratio of the molecular weight of water to a suitably defined average molecular weight of dry air. Since $\varepsilon < 1$, the specific volume of moist air is greater than that of dry air at the same temperature and pressure, and thus the virtual temperature is greater than the actual temperature. A balloon filled with moist air will rise through dry air at the same temperature. Unfortunately, this is not a strong enough effect to be of use to balloonists, but it is important over tropical oceans: Evaporation of surface liquid water into air increases is specific humidity making it lighter and thus destabilizing the boundary layer. *Much of the buoyancy flux in the boundary layer over tropical oceans is owing to evaporation rather than sensible heat flux.*

Because r is conserved in the absence of evaporation and condensation, we can define a conserved variable called the *virtual potential temperature*:

$$\theta_v = T_v\left(\frac{p_0}{p}\right)^{R_d/c_p}. \tag{4.10}$$

(Technically, the constants that appears in the exponent of (4.10) should be mixing ratio-weighted combinations of the gas constants and heat capacities of dry air and water vapor, but by a happy accident, the ratio of these weighted parameters is nearly equal to the ratio of their dry values.) Likewise, buoyancy fluctuations can be written

$$B = g\frac{\theta_v'}{\overline{\theta_v}}. \tag{4.11}$$

All the solutions for the convective boundary layer discussed in Chapter 2, section 2.3, should be re-written replacing actual by virtual temperatures and potential temperatures.

4.3 Aerodynamic flux formulae

Specification of the bulk heat sink and momentum source of the fluid is equivalent to specifying the surface fluxes of heat and momentum only if the system is in equilibrium. If the system is not in equilibrium, or if one only knows the wind speed and temperature, it is better to try to relate the surface fluxes to quantities like the surface temperature, atmospheric temperature, and wind speed.

This is particularly straightforward if we can measure quantities at an altitude (or choose a model level) that is much larger than the roughness length but much smaller than L. This will be usually be possible except where background winds are very light and/or the surface buoyancy forcing is very large (for example, over a desert in daytime). Standard measuring altitudes for surface meteorological stations around the world is, for example, 10 m. If these conditions are met, we can assume we are in the mechanical limit of turbulence generation and write a relation for the surface stress τ by algebraically inverting (4.2):

$$\tau \equiv \rho u^{*2} = \frac{k^2}{\left(\ln\left(\frac{z_m}{z_0}\right)\right)^2}\rho\overline{U_m}^2 \equiv C_D\rho\overline{U_m}^2, \tag{4.12}$$

where the subscript m denotes quantities at the measurement altitude and

$$C_D \equiv \frac{k^2}{\left(\ln\left(\frac{z_m}{z_0}\right)\right)^2} \tag{4.13}$$

is a non-dimensional number known as the *drag coefficient*, which is clearly a function of the roughness length and the measurement altitude. This can easily be generalized to flows in an arbitrary direction:

$$\boldsymbol{\tau} = C_D\rho\,|\,\mathbf{V}_m\,|\,\mathbf{V}_m, \tag{4.14}$$

where $\mathbf{V}_m$ is the horizontal velocity vector at the measurement altitude. We can also integrate in the vertical and then invert (4.6), using the empirical function Ψ_T given by (4.8) in the limit of large L/z, to relate the surface buoyancy flux to the difference in virtual potential temperature between the surface itself and the measurement altitude z_m:

$$F_B = C_T\,|\,\mathbf{V}_m\,|\,g\beta\left(\theta_{v0} - \theta_{vm}\right), \tag{4.15}$$

where θ_{v0} is the virtual potential temperature of the surface and C_T is the surface exchange coefficient for heat and is related to the constants we have previously defined:

$$C_T = \frac{\sqrt{C_D}}{c_1 (13k)^{1/3} \ln\left(z_m / z_0\right)}. \tag{4.16}$$

As with the drag coefficient, this nondimensional coefficient is a function of the measurement altitude and the surface roughness length.

Fluxes of other passive tracers should obey relations similar to (4.15), as long as the measurement altitude is much larger than the surface roughness length but much smaller than L.

The relations (4.14) and (4.15), and similar relations for passive tracers, are collectively known as aerodynamic flux formulae. They are straightforward to apply to field measurements to estimate surface fluxes, but in models it must always be remembered that quantities like $\mathbf{V}_m$ and θ_{vm} are themselves functions of the surface fluxes, so the fluxes must be calculated iteratively. This is a consequence of the fact that such quantities are not true externals of turbulent boundary layers. In addition, over the ocean the surface roughness depends on the presence and amplitude of surface waves and capillary waves, and will also vary with the direction of the wind relative to the orientation of the surface waves. In spite of these complications, the aerodynamic flux formulae enjoy widespread use, and when we come to discuss tropical cyclone physics, we will see that they depend crucially on turbulent exchanges of enthalpy and momentum between the boundary layer and the surface.

4.4 Clear boundary layers

The atmosphere sufficiently far away from the surface is nearly always stably stratified to vertical displacements that do not involve phase change of water. In the tropics, this is mostly because deep moist convection, even if it is distant, keeps the virtual temperature lapse rate close to neutral to moist displacements (see Chapter 3, section 3.2), and such a lapse rate is stable to reversible vertical displacements in which water does not change phase.

When stably stratified fluid flows over the earth's surface, the resulting shear causes a turbulent boundary layer to form; likewise, a positive surface buoyancy flux will result in convection that forms a turbulent layer.

As the turbulent eddies impinge on the stably stratified fluid above the turbulent layer, they engulf some of that fluid, which then becomes part of the turbulent layer. This process is called *entrainment*, similar to the later entrainment that occurs with deep moist convection (Chapter 3).

As air is entrained into the boundary layer from above, the layer grows, and the rate of growth can be described by an *entrainment velocity*, w_e. Over land, the growth of the boundary layer is often limited by the duration of solar heating of the surface; after the sun sets the source of turbulent energy vanishes (unless there is enough background wind) and the boundary layer collapses. Over the sea, the depth of the boundary layer is usually limited by radiatively induced

subsidence in the overlying air. If extensive clouds form at the top of the boundary layer, though, phase changes of water and strong radiative cooling from the tops of the clouds can dramatically alter the properties and growth of the layer. Here we first consider boundary layers that, for whatever reason, are dry enough that water does not condense. We also assume that, as is typical over the oceans, there is a positive buoyancy flux that is strong enough that the Obukhov length is less than the overall depth of the boundary layer.

The presence of another important length scale, the overall boundary layer depth, formally obviates the dimensional arguments that underlie the Monin-Obukhov scaling. In particular, the largest turbulent eddies span the whole boundary layer, so that, for example convection may have a larger effect on the surface winds than would be the case with the Monin-Obukhov scaling. nevertheless, observations show that the scaling relations work quite well up to about the depth corresponding to the Obukhov length, L. This layer, in which thermodynamic variables and momentum may vary relatively rapidly, is known as the *surface layer*. Above that, the boundary layer turbulence is mostly generated by buoyancy, and the conserved buoyancy variable θ_v, is nearly constant with height. Other conserved variables, such as the water vapor mixing ratio r may have weak but detectable mean gradients, however, and therefore we prefer to refer to this layer as the *convective layer* rather than the more conventional term *mixed layer*. Near the top of the boundary layer there are usually sharp gradients in momentum and conserved variables; in this layer, called the *entrainment zone*, quiescent air from above the boundary layer has a strong influence. At upper boundary of the entrainment zone the transition from turbulence to quiescence may be quite abrupt. The overall structure of the clear boundary layer is illustrated by Figure 4.1, which also shows typical physical altitudes of the various transitions over tropical oceans.

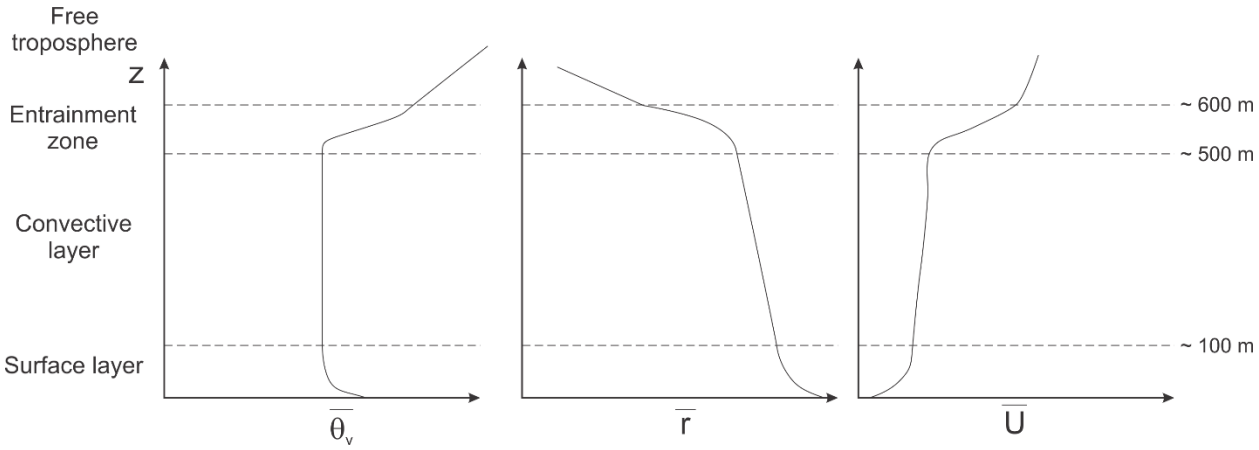

Figure 4.1: Schematic vertical structure of clear boundary layers over the ocean, showing mean virtual potential temperature (left), water vapor mixing ratio (middle) and wind speed (right). Typical altitudes of the transitions are shown at far right.

An important semi-empirical formulation of the entrainment velocity was developed by Lilly (1968), who assumed that some fraction of the turbulent kinetic energy generated by the surface buoyancy flux is used to increase the potential energy of entrained air. Put another way, the work done against buoyancy in entraining higher virtual potential air from above the boundary layer is provided by part of the positive buoyancy flux from the surface:

$$\overline{w_t' B_t'} = -a\overline{w_0' B_0'}, \tag{4.17}$$

where the term on the left represents the turbulent buoyancy flux at the top of the layer and the term on the right is the surface buoyancy flux multiplied by a constant a. From field measurements, a typical value of a is 0.2.

In turn, we can model the entrainment buoyancy flux as the product of an entrainment velocity, w_e, and the jump $\Delta\overline{B}$ in mean buoyancy across the entrainment zone:

$$\overline{w_t' B_t'} = -w_e \Delta\overline{B}. \tag{4.18}$$

Combining (4.17) with (4.18) yields a formulation for the entrainment velocity:

$$w_e = \frac{a\overline{w_0' B_0'}}{\Delta\overline{B}} = \frac{a\overline{w_0' \theta_{v0}'}}{\Delta\overline{\theta_v}}. \tag{4.19}$$

The second relation on the right of (4.19) results from expressing buoyancy in terms of virtual potential temperature.

The entrainment velocity together with the free tropospheric clear-sky subsidence rate determine the growth of the boundary layer depth:

$$\frac{\partial h}{\partial t} = w_e - w_{rad}, \tag{4.20}$$

in which h is the boundary layer depth, and w_{rad} is the clear-sky subsidence velocity, defined positive downward here. This latter quantity is related to the radiative cooling rate $\dot{Q}_{cool}$ by

$$w_{rad} = \frac{\dot{Q}_{cool}}{S}, \tag{4.21}$$

where S is the vertical gradient of dry static stability.

For a set surface buoyancy flux, the entrainment velocity decreases as the boundary layer depth grows. Referring to the left panel of Figure 4.1, note that the jump in $\overline{\theta_v}$ across the entrainment zone increase as the boundary layer depth increases, because the vertical gradient of $\overline{\theta_v}$ in the free troposphere is positive. Thus, from (4.19), w_e decreases. Eventually it will become as small as the radiative subsidence velocity and the boundary layer will cease growing.

Note that the surface virtual potential temperature flux in this conceptual model is positive while the turbulent flux of virtual potential temperature into the boundary layer from the top is negative; both of these act to increase the mean θ_v of the boundary layer. In equilibrium, this must be balanced by internal sinks, including radiative cooling and, under some conditions, horizontal advection of cooler air.

Also note from the right panel of Figure 4.1 that the mean wind usually has a shear across the entrainment zone. If this is such that the Richardson Number, defined

$$Ri \equiv \frac{\frac{g}{\theta_v}\frac{\partial \theta_v}{\partial z}}{\left|\frac{\partial \mathbf{V}}{\partial z}\right|^2} \tag{4.22}$$

is smaller than a critical value, then instabilities driven by the local wind shear can amplify and enhance the turbulent entrainment into the top of the boundary layer, causing it to grow faster and/or become deeper.

To be self-consistent, the solution for clear-sky boundary layers must be everywhere sub-saturated with respect to water vapor, otherwise clouds will develop and can dramatically alter the properties of the boundary layer, as explored in the next sections.

4.5 Stratocumulus-topped boundary layers

When air near the top of the boundary layer is moist enough to approach 100% relative humidity, clouds form. If the cloudy air is stable to reversible displacements above the top of the boundary layer, the cloudy air is trapped in the boundary layer, and depending on the particular circumstances, the clouds may form a nearly solid layer of stratocumulus or may break down into more isolated shallow cumulus clouds. Here we briefly review stratocumulus-topped boundary layers. Even though the clouds are relatively thin, they cover extensive areas of subtropical (and also arctic) oceans and play a large role in climate by contributing much of the planet's albedo. An example of boundary layer stratocumuli seen from above is provided in Figure 4.2.

The general structure of the cloud-topped boundary layer is similar to that of clear boundary layers (see Figure 4.3), but there are important differences. First, the relevant conserved variables are the total water mixing ratio r_T, which is conserved provided there is no precipitation, and the *liquid water density potential temperature*, defined

$$\theta_{\rho l} \equiv T_\rho \left(\frac{p_0}{p}\right)^{R_d/c_p} \exp\left(\frac{-L_v r_l}{c_p T}\right), \tag{4.23}$$

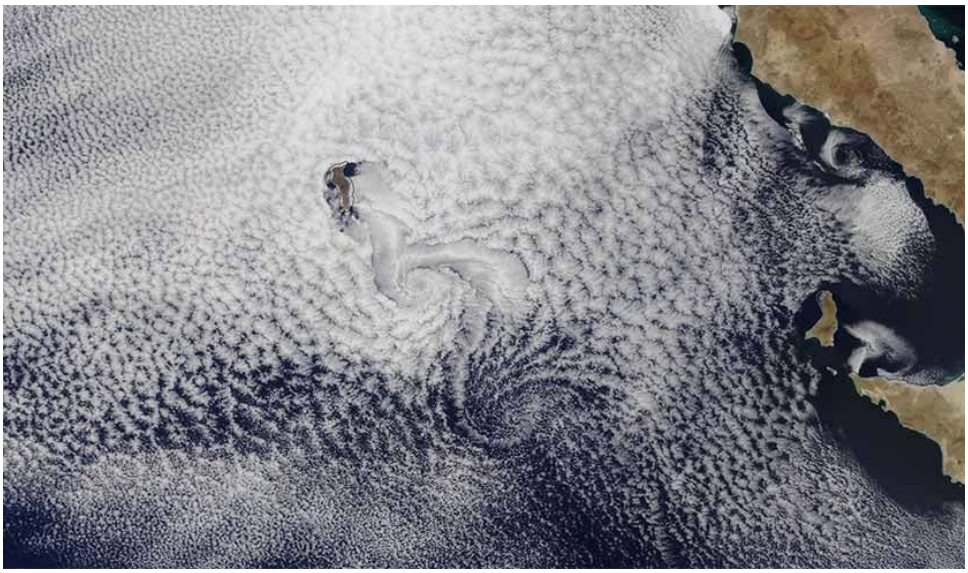

Figure 4.2: Boundary layer stratocumuli off Mexico's Baja California coast, on September 12th 2018, as seen from satellite. The northwesterly flow past Isla Guadaloupe is creating a vortex street to the southeast of the island.

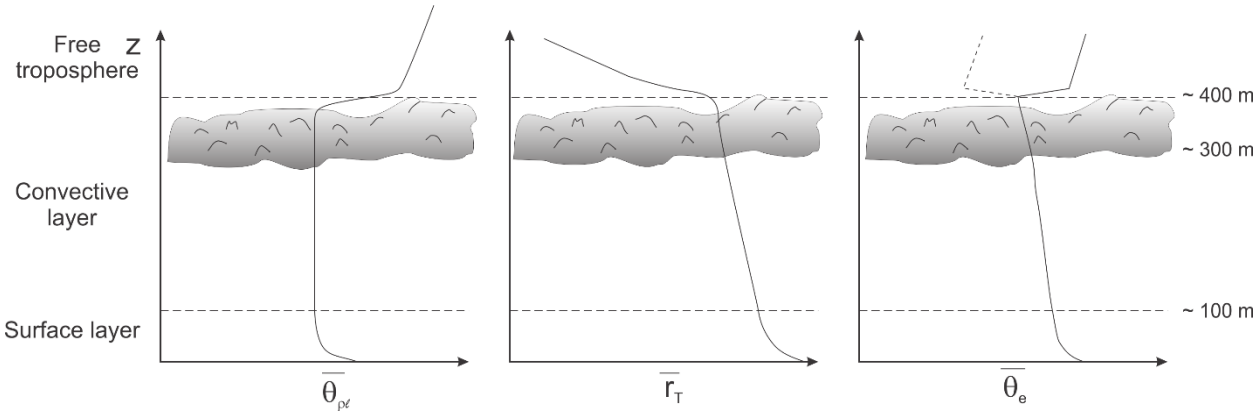

Figure 4.3: As in Figure 4.1 but for stratocumulus-topped boundary layers. The left panel shows the liquid water virtual potential temperature, the center panel shows the total water mixing ratio, and the right panel shows the equivalent potential temperature. The dashed line in the right panel shows and alternative θ_e profile above the boundary layer.

where T_ρ is the density temperature defined by (3.9) and r_l is the liquid water mixing ratio. Note that (4.23) reduces to the virtual potential temperature in the absence of liquid water. Also note that in Figure 3.2 we have omitted the entrainment layer, which tends to be very thin in stratocumulus-topped boundary layers.

Another conserved variable, absent radiative heating, is the equivalent potential temperature, θ_e, a typical profile of which is shown in the right panel of Figure 4.3. For reasons we will discuss shortly, two alternative profiles of θ_e are shown above the boundary layer.

The top of stratocumulus layers is usually marked by abrupt changes in conserved variables and in momentum, but these variables are continuous through cloud base. The stratocumulus, if they are thick enough, may produce drizzle, which can play a role in transitioning the layer toward a trade cumulus boundary layer, as will be discussed in the next section.

In addition to the presence of clouds and possible drizzle, there are two aspects of cloudy boundary layers that distinguish them from other kinds of boundary layer. Most importantly, the large infrared opacity of the clouds gives rise to a strong jump in infrared flux, producing a spike in radiative cooling at the cloud top. This cooling at the layer top is an important source of convective turbulence in the boundary layer. The clouds absorb solar radiation during the day, and this heating may offset the infrared cooling enough to thin and/or cause breaks in the clouds.

Moreover, if the overlying atmosphere in sufficiently dry and not too warm, then the jump in θ_e across the top of the layer may be negative, a possibility illustrated in Figure 4.3. When this happens, air mixed into the boundary layer from above will have a lower value of θ_e than the surrounding cloudy air, and if enough liquid water evaporated into the mixture to saturate it, it will have a negative temperature anomaly and may be negatively buoyant. (In contrast, air entrained into clear boundary layers will always be positively buoyant.) This can cause the cloud top to be unstable; this is known as *cloud top entrainment instability* and enhances the production of turbulence in the layer.

Advective drying of the free troposphere above stratocumulus-topped boundary layers will enhance the aforementioned instability and also the jump in infrared flux across clouds top, both of which will increase the turbulence kinetic energy of the boundary layer. On the other hand, the jump in buoyancy across the boundary layer top is likely to increase, and these act in opposite directions on the entrainment velocity (see (4.19)). The drying will also be associated with a reduction in the radiative cooling of the free troposphere, reducing the clear-sky subsidence velocity. From (4.20) the layer may either deepen or become shallower, depending on the relative importance of the processes. All other things being equal, a deeper boundary layer would be more likely to have clouds at its top, but on the other hand the air being entrained from the free troposphere may be dryer, working in the opposite direction. This illustrates the complexity of the response of stratocumulus layers to changing environmental conditions.

On time scales of a few years and greater, stratocumulus-topped boundary layers, by shielding the surface from sunlight and thereby keeping it cold, may be self-preserving.

Over warmer surfaces, stratocumulus-topped boundary layers may transition toward layers containing scattered cumulus clouds. The nature of this transition is explored in the next section.

4.6 Transitioning boundary layers

Stratocumulus-topped boundary layers generally occur over cold water, often resulting from upwelling in the ocean. As boundary layer air moves westward and equatorward following the general flow of the trade winds, it encounters increasing sea surface temperatures, resulting in stronger enthalpy and buoyancy fluxes from the surface. The cloud-topped boundary layer grows deeper, entrainment increases, and the higher temperatures and deeper boundary layer yield higher liquid water concentrations in the clouds, increasing the probability and intensity of drizzle. The higher θ_e of the boundary layer makes more likely a negative jump in θ_e across the boundary layer top.

The depletion of net water concentration by drizzle and further depletion by increased entrainment from above lead to drier downdrafts in the cloud layer, and consequently to higher lifted condensation levels in the downdrafts. At levels between the LCLs of updrafts and downdrafts, the air is likely to have a moist adiabatic lapse, which is stable to the downward-moving unsaturated air. The asymmetry between nearly neutral stability to saturated updrafts and strong stability to unsaturated downdrafts concentrates the updrafts and broadens the downdrafts.

The result of this asymmetry is the development of cumuliform clouds in the layer between the LCLs of the upward moving air from the surface layer and the downward moving air from the top of the boundary layer, as illustrated on Figure 4.4. The stratocumulus layer becomes broken and partially decoupled from the surface, with the cumulus clouds being the agents of coupling. As illustrated in the figure, there are now four distinct layers: The surface layer, the subcloud layer (which includes the surface layer), the convecting layer, and the stratocumulus layer.

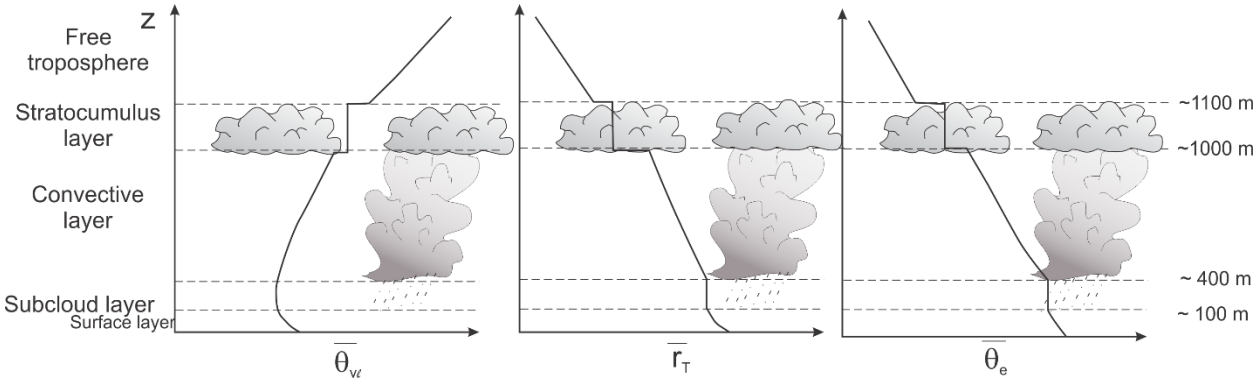

Figure 4.4: Vertical structure of a stratocumulus-to-cumulus transitioning boundary layer. Liquid water virtual potential temperature is shown at left, the total water mixing ratio in middle, and the equivalent potential temperature at right. The subcloud layer consists of a surface layer and an unsaturated convecting layer driven by the surface buoyancy flux. Cumulus clouds extend though the convecting layer and penetrate the stratocumulus layer, which is internally well mixed.

The subcloud layer above the surface layer is generally well mixed in the vertical, as is the stratocumlus layer, but the convecting layer usually is stably stratified to dry convetion and has slowly decreasing total water concentration with height. There may or may not be small jumps in thermodynamic properties across the base of the starocumulus layer.

In this configuration, the stratocumuus layer is supplied with water by the cumulus clouds, which extend vertically into the layer and may ocassionaly overshoot a small distance into the free troposphere. The elevated stratocumulus layer loses water mostly by entraining dry air from above but sometimes also by drizzle, and the cumuli many be lightly precipitating. Radiative cooling of the stratocumulus tops is an important source of turbulence in the elevated cloud layer.

Figure 4.5 is a photo of a transitioning boundary layer taken from the surface.

Figure 4.5: Showing a transitioning boundary layer, with shallow cumuli penetrating a stratocumulus layer that is otherwise decoupled form the surface.

Transitioning boundary layers are widespread in the subtropics, and the fractional area covered by clouds can vary widely from around 10% to nearly 100%, so they also important in determining local and plantary albedo.

4.7 Trade cumulus boundary layers

Over warmer water but away from regions of deep moist convection, transition boundary layers give way to yet deeper boundary layers populated by shallow cumulus clouds unaccompanied by extensive stratocumulus layers near their tops. Since these clouds are frequent in the trade wind[2] belts, they are frequently referred to as “trade cumuli”. They are often weakly precipitating, and anyone who has spent time in the tropics will be familiar with the sudden but brief showers they may produce. Figure 3.2 shows a nice example of a trade cumulus clouds.

[2] The “trade winds” are belts of easterly winds found through much of the tropics and are so called because they were used in the Age of Sail to facilitate maritime trade mostly between Europe and the East and West Indies. We will explore their underlying dynamics in Chapter 6.

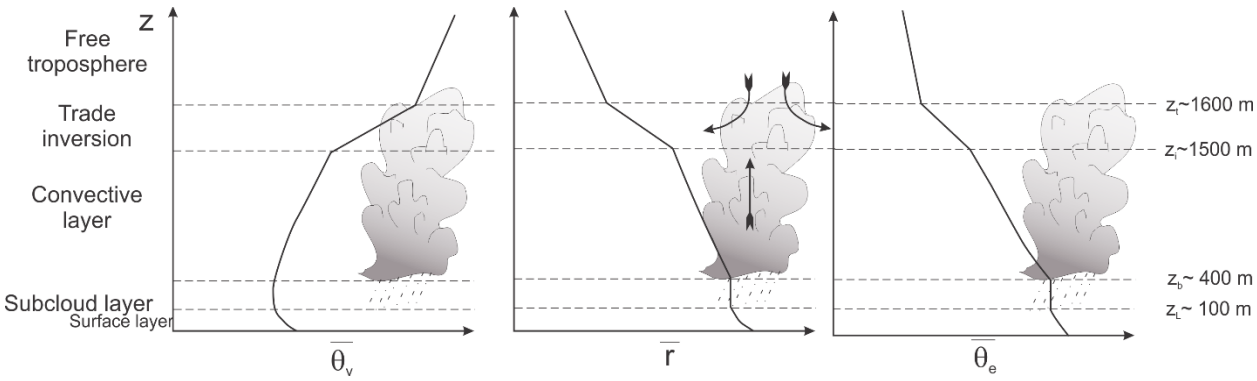

Figure 4.6: Vertical thermodynamic structure of a trade cumulus boundary layer, showing mean virtual potential temperature (left), water vapor mixing ratio (center) and equivalent potential temperature (right). The middle panel also shows typical air trajectories in the cumulus clouds.

The thermodynamic structure of trade cumulus boundary layers is illustrated in Figure 4.6. The layer bearing the cumulus clouds is stably stratified and is capped by a “trade inversion” in which the virtual potential temperature increases sharply, giving way to the more modest increase with height typical of the tropical free troposphere. Likewise, water vapor mixing ratio and θ_e decrease with altitude in the convective layer and often more sharply in the inversion.

Entrainment from the free troposphere is an essential process in trade cumulus layers, as in other boundary layers, but much of the entrainment occurs into the tops of the cumuli, even though they occupy a relatively small fractional area. As the cumuli poke upward into the inversion layer, they turbulently entrain air from the free troposphere. This air is typically very dry, and since the liquid water virtual potential temperature (defined by (4.23)) is smaller in the clouds than in the free troposphere (unless the clouds are strongly precipitating), any mixture that contains little or no liquid water will have a density temperature that is smaller than that of the cloud, and will thus be negatively buoyant. This cloud top entrainment instability results in fairly large entrainment into the tops of the clouds, and the mixtures typically detrain into the inversion. Over the lifetime of the cloud, there is a net downward cumulus mass flux in the trade inversion, while there is a net upward flux in the convecting layer, as illustrated in the middle panel of Figure 4.6.

For a strictly non-precipitating cloud, there can be no net latent heat release over the lifetime of the cloud, and this, together with the virtual potential temperature structure of the trade cumulus boundary layer, constrains the relative magnitudes of the downward mass flux at the clouds top and the upward mass flux in the cloud layer. Let the former be defined as M_d (defined positive downward) and the latter as M_u. Then

$$\int_{z_b}^{z_i} \rho M_u \frac{\partial \theta_v}{\partial z} = \int_{z_i}^{z_t} \rho M_d \frac{\partial \theta_v}{\partial z}, \tag{4.24}$$

where z_b, z_i, and z_t are the respective altitude of cloud base, the base of the inversion, and the top of the inversion (see Figure 4.6). The absence of latent heating also means that the radiative cooling of the cloud layer must be compensated by warming by large-scale subsidence. This shows that there must be substantial net downward motion in the inversion

layer; indeed, the cloud-top cooling maintains the strong virtual potential temperature gradients across the inversion.

But trade cumuli often *do* precipitate. It is important to recognize, from (4.23), that *precipitation is a source of liquid water density potential temperature*. When the cumuli precipitate, they gain $\theta_{\rho l}$ and this decreases the degree of cloud top detrainment instability because the mixtures will not be as negatively buoyant, owing to less condensed water available for evaporation. With lowered entrainment, the depth of the boundary layer will decrease (see 4.20), and as the clouds become shallower, they become less likely to precipitate. Thus there may be a self-regulation mechanism in play that keeps the cumuli, on average, just barely precipitating, and holds the depth of the layer such that the clouds are just barely deep enough to develop precipitation.

The evaporation of rain falling from trade cumuli cools the air and the cold pools spread out as density currents. The interaction of these cold pools with surrounding air, with the surface, with ambient wind shear and with convection can result in intricate and varied forms of mesoscale organization, as is apparent in Figure 3.3. The physics governing this organization is only now beginning to be understood.

While the clouds in trade cumulus boundary layers occupy a small fractional are a relative to stratocumulus and transitioning boundary layers, they still contribute non-negligibly to planetary albedo as they occupy large areas of the tropics and sub-tropics, and both the clouds and the humidity of these layers have important influences on radiative transfer.

4.8 Summary

In the tropics, boundary layers are defined, as elsewhere, as layers in which turbulent exchange between the atmosphere and underlying surface is important, and the turbulence can include convective clouds. They may occupy between 5% and 20% of the mass of the atmosphere and may contain much of the water vapor of the atmosphere, which together with the clouds, make them important in radiative as well as turbulent exchanges. Boundary layers may be clear, topped with stratocumulus clouds, or populated with trade cumuli, but large regions of the subtropics are in a state of transition between stratocumulus and trade cumulus regimes. These transitions are important to understand and predict and they greatly affect albedo. The currently poor ability of global climate models to simulate stratocumulus layers and transitioning boundary layers is considered a major (and perhaps *the* major) source of uncertainty in climate projections.

Figure 4.7 shows a satellite-derived snapshot of clouds over the eastern and central North Pacific with an attempt to visually delineate the various kinds of boundary layers discussed in this chapter. It is not always easy to identify cloud types from satellite imagery; for example, it may be difficult or impossible to see cumulus growing upward into a stratocumulus layer. Nevertheless, the diagram shows that the regions occupied by deep convection (and these are liberal estimates) cover a small region compared to the areas in which most clouds are in the boundary layer. Note also that even the trade cumulus regimes are noticeable brighter than the clear regions, indicating that the albedo due to the cumuli is not negligible.

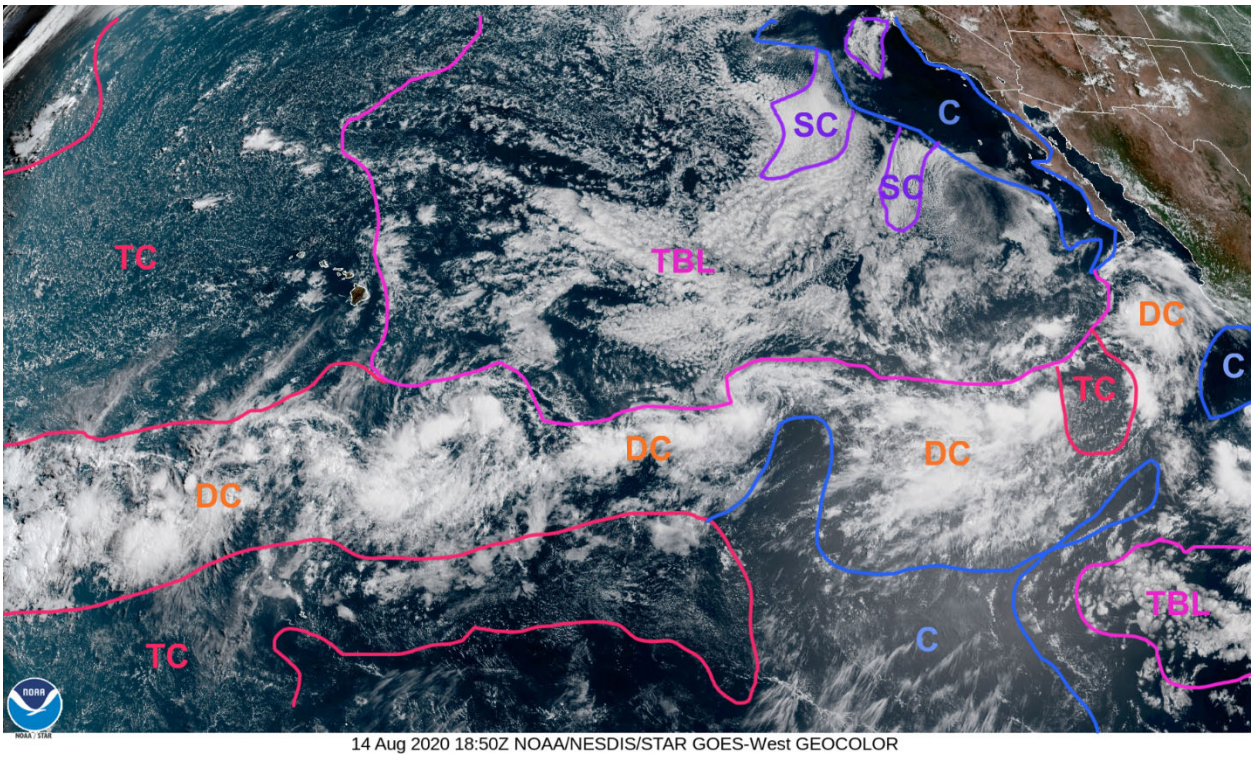

Figure 4.7: Visible satellite imagery from 18:50 GMT on 14 August 2020, showing clouds over the eastern and central subtropical North Pacific. Colored overlays are subjective estimates of the various regimes: "C" for "clear", "SC" for "stratocumulus-topped boundary layers", "TBL" for "transitioning boundary layers", "TC" for "trade cumulus boundary layers", and "DC" for "deep convection".

A schematic cross-section showing the progression of regimes as one travels from cold water upwelling regions near coastlines bounding the eastern sides of oceans down into the deep tropics is presented in Figure 4.8.

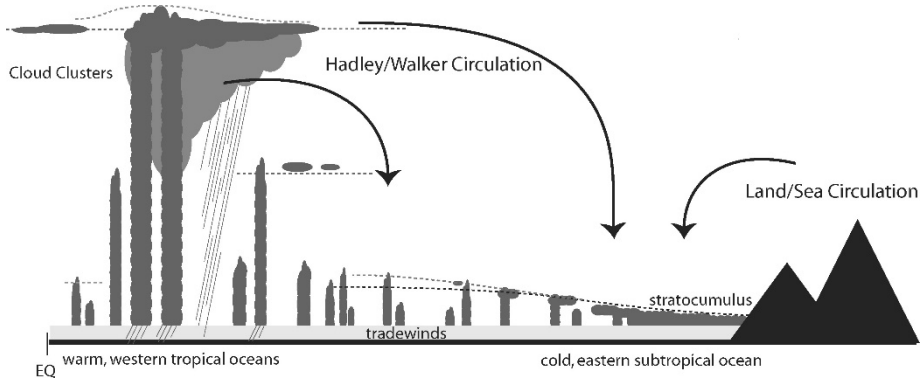

Figure 4.8: Showing the transition of boundary layer regimes from stratocumulus layers over cold, subtropical eastern oceans (right) to deep convective regimes over warm tropical oceans (left).

Travelling from cold ocean water on the right to very warm tropical oceans on the left, the boundary layer deepens from a few hundred meters to a few kilometers and transitions from a completely overcast stratocumulus-topped layer to a trade cumulus boundary layer and finally to a relatively narrow deep convective regime.

Boundary layers are interesting but complex features of the tropical atmosphere and much of what we will discuss in forthcoming chapters depends on knowledge of their behavior. We have only skimmed the surface of their physics here, omitting important contributions such as planetary rotation and horizontal advection, and they are prominent subjects of ongoing research. The reader is encouraged to consult more thorough treatment of boundary layers such as the classic text by Stull (1988) and a recent and comprehensive review (LeMone et al., 2019).

References

Businger, J. A., and Y. I. J. C. Wyngaard, and E. F. Bradley, 1971: Flux profile relationships in the atmospheric surface layer. *J. Atmos.. Sci.*, **28,** 181-189.

Dyer, A. J., 1974: A review of flux-profile relations. *Bound. Layer Meteor.*, **1,** 363-372.

LeMone, M. A., and Coauthors, 2019: 100 years of progress in boundary layer meteorology. *Meteorological Monographs*, **59,** 9.1-9.85, doi:10.1175/amsmonographs-d-18-0013.1.

Lilly, D. K., 1968: Models of cloud-topped mixed layers under a strong inversion. *Quart. J. Roy. Meteor. Soc.*, **94,** 292-309.

Monin, A. S., and A. M. Obukhov, 1954: Basic laws of turbulent mixing in the surface layer of the atmosphere. *Tr. Akad. Nauk. SSSR Geophiz. Inst.*, **24,** 163-187.

Stull, R. B., 1988: *An introduction to boundary layer meteorology .* Kluwer Acad. Publ., Boston, 666 pp. pp., translator.